



Title	Gigantic chiroptical enhancements in polyfluorene copolymers bearing bulky neomenthyl groups : importance of alternating sequences of chiral and achiral fluorene units
Author(s)	Watanabe, Kento; Koyama, Yasuhito; Suzuki, Nozomu; Fujiki, Michiya; Nakano, Tamaki
Citation	Polymer chemistry, 5(3), 712-717 https://doi.org/10.1039/c3py01442h
Issue Date	2014-02-07
Doc URL	http://hdl.handle.net/2115/57950
Type	article (author version)
File Information	PolymChem_5_Watanabe_r5-1.pdf



[Instructions for use](#)

COMMUNICATION

Gigantic Chiroptical Enhancements in Polyfluorene Copolymers Bearing Bulky Neomenthyl Group: Importance of Alternating Sequence of Chiral and Achiral Fluorene Units

Cite this: DOI: 10.1039/x0xx00000x

Received 00th January 2012,
Accepted 00th January 2012

DOI: 10.1039/x0xx00000x

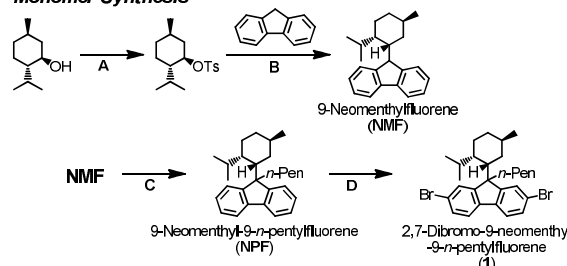
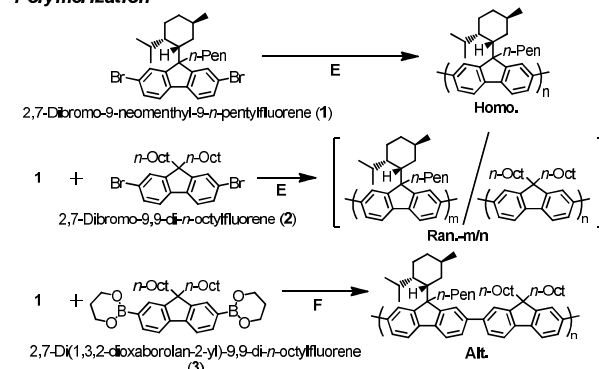
Kento Watanabe,^a Yasuhito Koyama,^a Nozomu Suzuki,^b Michiya Fujiki,^b and Tamaki Nakano*^a

www.rsc.org/

An alternating copolymer consisting of achiral and chiral units emits remarkably efficient CPL on photo-excitation. Main-chain twist bias is enhanced by thermal annealing by the factor of 10^4 in the ground state. Anisotropy factor of the polymer in excited states is greater by approximately an order of magnitude compared with that in the ground state.

Fluorescent and phosphorescent organic polymers are an important class of materials from both basic photophysical and application-oriented views. Emission properties shed light on chiral structures in excited states and also can be applied for organic light-emitting diodes (OLEDs). As applied materials, emitting polymers have advantages that emission properties can be modified through molecular designs because they are inherently light-weight and flexible and that they can be readily fabricated by solution processes.¹ Among various polymers in this class, those emitting circularly polarized light (CPL) are of particular interest because of their potential for photonic devices such as 3D displays and energy-efficient backlights for LC displays.²⁻⁴ CPL-emitting polymers extensively studied so far include derivatives of poly(*p*-phenylenevinylene),⁵ polyfluorene,⁶ poly(*p*-phenyleneethynylene),⁷ polysilane,⁸ polythiophene,⁹ a hyperbranched fluorenevinylene polymer,¹⁰ poly(dibenzofulvene),¹¹ and cyclophane-based polymers.¹² In most of these examples, anisotropy factor in CD spectra ($g_{CD} = 2(\epsilon_L - \epsilon_R)/(\epsilon_L + \epsilon_R)$, where ϵ_L and ϵ_R are molar absorption coefficients of left-handed and right-handed CPLs, respectively) and that in CPL emission ($g_{CPL} = 2(I_L - I_R)/(I_L + I_R)$, where I_L and I_R are emission intensities of left-handed and right-handed CPLs, respectively) are similar. This means that chiral structure in the ground state is similar to that in photo excited states.

Most of all experimental results reported so far lead to an idea that a material with a high g_{CD} is necessary to achieve a high g_{CPL} . On the other hand, we recently found that, in the green-emitting hyperbranched fluorenevinylene polymer bearing bulky neomenthyl group as chiral source, the absolute magnitude of g_{CPL} , $|g_{CPL}|$, reached the order of 10^{-1} , although the corresponding absolute

Monomer Synthesis**Polymerization**

Scheme 1 Monomer synthesis and polymerization. Reagents and conditions: (A) 2 eq. of *p*-toluenesulfonyl chloride, in pyridine/ CHCl_3 (1/2, v/v), r.t., overnight, 87%; (B) 1 eq. of 9-fluorenyllithium, in THF, -78°C to reflux, overnight, 22%; (C) 1) 1.5 eq. of *n*-butyllithium/*n*-hexane, in THF, 0°C 2 h; 2) 1.5 eq. of *n*-pentyl iodide, in THF, r.t., overnight, 92%; (D) 2.5 eq. of Br_2 , 1.2 mol% of I_2 , in CH_2Cl_2 , r.t., 1.5 h, 85%; (E) 1) 1 eq. of magnesium, in THF, 60°C , 1 h; 2) 2 mol% of $\text{Ni}(\text{dppp})\text{Cl}_2$, in THF, 60°C , 24 h; (F) 10 mol% of $\text{Pd}(\text{PPh}_3)_4$, 7 eq. of K_2CO_3 , in 1,4-dioxane/water (5/2, v/v), 110°C , 2.5 h.

^aCatalysis Research Center and Graduate School of Chemical Sciences and Engineering, Hokkaido University, Sapporo 001-0021, Japan; Fax: +81-11-706-9156; E-mail: tamaki.nakano@cat.hokudai.ac.jp

^bGraduate School of Materials Science, Nara Institute of Science and Technology, 8916-5 Takayama, Nara 630-0101, Japan

† Electronic Supplementary Information (ESI) available: [details of any supplementary information available should be included here]. See DOI: 10.1039/c000000x/

Table 1 Synthesis of optically active polyfluorene derivatives bearing neomenthyl group in the side chain^a.

Run	Symbol	Monomer	[1]/[2 or 3] (mol%) in feed	Conv. ^b (%)	MeOH-insoluble part					
					Yield (%)	[NPF]/[DOF] in polymer ^c	M_n (M_w/M_n) ^d (vs. PSt)	M_n (M_w/M_n) ^e (VISC-RALS)	$[\alpha]$ ^f (deg)	α ^{e,g}
1	Homo.	1	100/0	98	77	100/ 0	11,800 (4.15)	10,400 (1.56)	-0.5	0.864
2	Ran.-9/1	1, 2	90/10	>99	72	91/ 9	19,500 (3.45)	10,000 (1.57)	-0.6	0.868
3	Ran.-1/1	1, 2	50/50	97	84	53/47	13,400 (4.17)	8,800 (1.70)	+0.6	0.890
4	Ran.-1/9	1, 2	10/90	92	84	14/86	18,400 (5.11)	16,400 (1.82)	+0.3	0.865
5	Alt.	1, 3	50/50	>99	72	50/50	25,300 (5.27)	22,300 (2.35)	+0.9	0.890

^aConditions: solvent = THF, temp. = 60 °C, time = 24 h, [monomer]₀ = 0.60 M, [Ni]₀ = 2.0 mol% (runs 1-4); solvent = 1,4-dioxane/H₂O (5/2, v/v), temp. = 110 °C, time 2.5 h, [monomer]₀ = 0.25 M, [Pd]₀ = 10 mol% (run 5). ^bDetermined by ¹H NMR spectra of reaction mixture. ^cDetermined by ¹H NMR spectra of the isolated polymers (Fig. S1). ^dDetermined by SEC (vs. PSt, in THF, r.t.). ^eDetermined by SEC-VISC-RALS (in THF, 30 °C). ^fSpecific rotation of the polymers measured in THF at r.t. (conc. = 4 g/dL, cell length = 1 cm). ^gMark-Houwink-Sakurada constant.

magnitude of g_{CD} , $|g_{CD}|$, is on the order of only 10^{-4} .¹⁰ For this system, chiral structure of the emitting species seems to be largely different from that in the ground state detected by CD spectra. Although details of CPL emission mechanism in this system are yet to be explored, the polymer in ref 10 is obviously characterized by the two chemical structural factors, *i.e.*, the bulky, cyclic neomenthyl side-chain group and the hyperbranched main chain.

To clarify the effect of neomenthyl group compared to linear systems, here we studied chiroptical properties of optically active copolymers consisting of 9-neomenthyl-9-*n*-pentylfluorene-2,7-diyl and 9,9-di-*n*-octylfluorene-2,7-diyl units in addition to a homopolymer of the chiral units. Although, as polyfluorene derivatives emitting CPL, a series of polymers having linear, chiral side chain were studied well,⁶ those having bulky, cyclic chirality source group have never been reported.

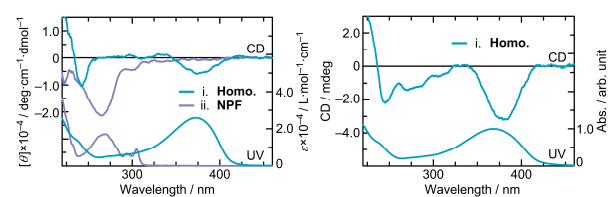
Chemical transformations and polymerizations conducted in this work are indicated in Scheme 1. *l*-Menthol as a source of neomenthyl group is an inexpensive chiral organic compound obtained from peppermint or other mint oils or synthesized on industrial basis from achiral myrcene via (*R*)-citronellal derived from an asymmetric isomerization of an allylic amine with Rh-BINAP catalyst.¹³ The chiral moiety of menthol can be readily embedded into fluorene via a reaction between menthyl tosylate and 9-fluorenyllithium where the absolute configuration at the 1-position of menthol moiety is inverted through an S_N2 substitution.¹⁴ The reaction thus results in 9-neomenthylfluorene, followed by synthesis of 2,7-dibromo-9-menthyl-9-*n*-pentylfluorene (**1**) as a new chiral monomer. Monomer **1** was homopolymerized by the Kumada-Tamao coupling¹⁵ or copolymerized with 2,7-dibromo-9,9-di-*n*-octylfluorene (**2**) in a random fashion by the Kumada-Tamao coupling or copolymerized with 2,7-di(1,3,2-dioxaborolan-2-yl)-9,9-di-*n*-octylfluorene (**3**) in the alternating fashion by the Suzuki-Miyaura coupling.¹⁶ The polymers possess 9-neomenthyl-9-*n*-pentylfluorene (NPF) unit as a chiral constituent and 9,9-di-*n*-octylfluorene (DOF) unit as an achiral constituent.

The conditions and results of polymerization are summarized in Table 1. All polymerization led to the desired polymers at high conversions. M_n 's of the products were of the order of 10^4 . In the random copolymerizations, the ratios of chiral NPF unit to achiral DOF unit were similar to nominal feed ratios of the corresponding monomers, suggesting that the two monomers have similar reactivities in copolymerization and that the polymers have a random distribution of the two units. In addition, Mark-Houwink-Sakurada constants of the polymers were in the range of 0.86–0.89, indicating

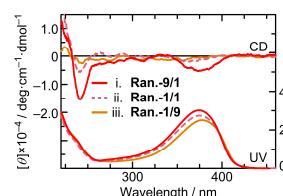
the chiral polymers prepared in this work adopt stiff conformations.¹⁷

The polymers showed only negligible specific rotations, regardless of chiral unit content and monomeric sequence. To obtain information on chiral structure of chromophores in the polymers in the ground state, CD and UV spectra of the polymers were measured in a tetrahydrofuran (THF) solution and in the solid state (cast film without any annealing process) as well as 9-neomenthyl-9-*n*-pentylfluorene (NPF) as a model of monomeric unit in a THF solution (Fig. 1A-F). The chiral homopolymer exhibited intense Cotton effects in the range of 350–400 nm in addition to shorter wavelength regions in THF (Fig. 1A). While, in THF, the random

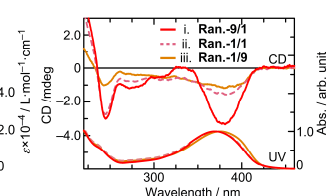
(A) Homo. and NPF in a THF solution (B) Homo. in film



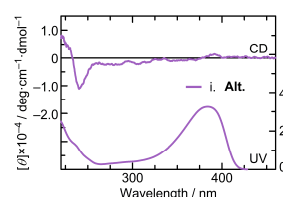
(C) Ran.-m/n in a THF solution



(D) Ran.-m/n in film



(E) Alt. in a THF solution



(F) Alt. in film

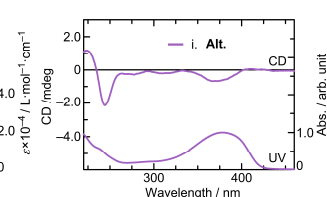
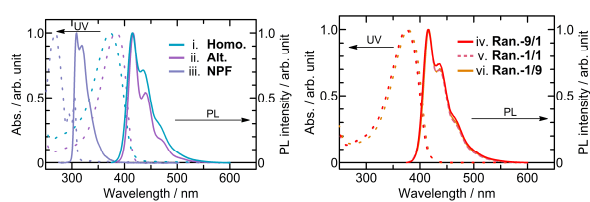


Fig. 1 UV and CD spectra of 9-neomenthyl-9-*n*-pentylfluorene (NPF) the homopolymer (Homo.) in a THF solution (A), HOMO. in film (B), the random copolymers (Ran.-9/1, -1/1, and -1/9) in a THF solution (C) and in film (D), and the alternating copolymer (Alt.) in a THF solution (E) and in film (F). For solutions; concentration was 1.0×10^{-5} M per residue and cell length was 1 cm. The film CD spectra were obtained by averaging four spectra taken at different orientations of the sample with regard to the incident light beam in order to minimize the effects of linear dichroism (see Fig. S2 for LD and UV spectra of the polymer films).

(A) Fluorescence in a THF solution



(B) Fluorescence in film

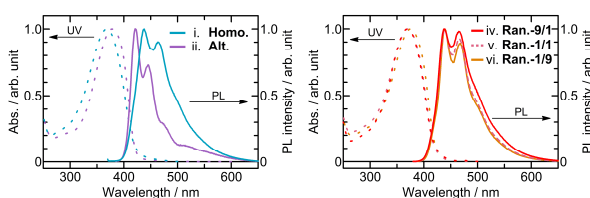


Fig. 2 Fluorescence (PL) spectra along with absorption spectra in a THF solution (A) and in film (B): the homopolymer (i), the alternating copolymer (ii), **NPF** (iii) and the random copolymers having 91 % (iv), 53 % (v) and 9 % **NPF** unit (vi); For solutions; concentration was 1.0×10^{-5} M per residue and cell length was 1 cm. λ_{ex} : in (A), 373 nm for all the polymers and 270 nm for **NPF**; in (B), 366 nm for all the polymers.

copolymers having 14 % and 53 % of chiral **NPF** units (**Ran.-1/9** and **Ran.-1/1** samples, respectively, in Table 1) did not show any clear CD band in this range, the one having 91 % of **NPF** units (**Ran.-9/1** sample in Table 1) did (Fig. 1C). Moreover, the alternating copolymer did not show clear CD in this range, in THF, either (Fig. 1E).

The absorption band in the 350–400 nm range is based on conjugation between monomeric units. This is supported by the fact that **NPF** does not absorb in this range. The polymer has conformational chirality based on twisting ability around single bonds connecting fluorene units, leading to detectable chiroptical properties.¹⁸ CD spectral intensity in this range may reflect a bias in the population of right- and left-handed twists between monomeric units. The $|g_{\text{CD}}|$ values for the homopolymer and the **Ran.-9/1** sample are of the order of 10^{-5} , which is typical of chiral π - π^* systems.

The spectra in Fig. 1A, C, and E may mean that 53 % of the chiral units is not enough to induce detectable conformational chirality in the polymer chain in solution. At a level of the chiral units higher than 53 %, the chance of two **NPF** units being connected in series is high. Hence, to induce a CD-detectable twist bias, steric repulsion exerted by neighboring bulky neomenthyl groups may be necessary.

The solution spectral properties are based on single chain chirality, not on chain aggregation in THF because CD spectral intensities and patterns were independent of solution concentration. This feature was confirmed by UV and CD spectra of the alternating copolymer taken at different concentrations (Fig. S3).

In contrast to the CD spectra in THF solutions, all film samples on a quartz plate fabricated by drop casting (film thickness: 0.33–1.31 μm) exhibited intense CD bands corresponding to the absorption bands (Fig. 1B, D, and F), indicating that main-chain twist bias is realized even for the polymers having 53 % or a less amount of chiral **NPF** units in the solid state. This means that intra-chain steric repulsion is stronger in the solid state or that inter-chain interaction/repulsion has an important role in twisting the main chain.

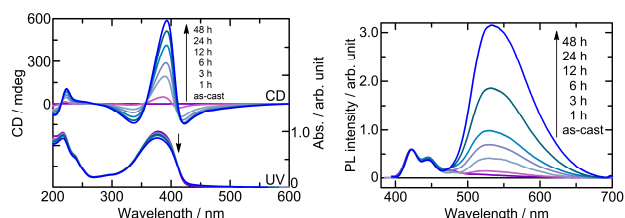


Fig. 3 Changes in CD-UV (left) and fluorescence (right) spectra of the alternating copolymer film on thermal annealing at 160 °C. λ_{ex} in (B) was 366 nm.

The $|g_{\text{CD}}|$ values in film were of the order of 10^{-4} – 10^{-5} and were over all higher than in a THF solution.

In addition, it is notable that, in solution, λ_{max} in absorbance of the alternating copolymer was 384 nm which was clearly longer than λ_{max} values of the other polymers (373–378 nm); the alternating copolymer may have a slightly smaller dihedral angle of the main-chain twist compared with the other polymers.

The polymer in a THF solution and in film emitted in visible region upon excitation. Fig. 2 compares the photoemission and UV-visible absorption spectra of the polymers and **NPF** as a monomeric unit model. In solution, all polymers emitted blue light showing λ_{em} at around 415 nm while **NPF** emitted at around 310 nm. The larger red-shift in polymer emission compared with **NPF** indicates that polymer emission arises from exciton extended over conjugated chromophore units. Internal fluorescence quantum yields (Φ_{Em}) of the polymers estimated using an integral sphere were in the range of 0.53–0.76, and that of **NPF** was 0.44 (See Table S2 for details). Quantum yields of the polymers are comparable to that of poly(9,9-di-*n*-octylfluorene-2,7-diyl) ($\Phi_{\text{Em}} = 0.63$),¹⁹ indicating that introduction of chiral side group does not alter basic emission mechanisms.

In the solid state, the alternating polymer behaved differently among the five polymers: λ_{max} of emission of the alternating copolymer had 422 nm, while those of the other polymers located at around 439 nm. This is interesting because λ_{max} of absorption was greatest for the alternating copolymer (Table S2). Differences in conformation between the alternating copolymer and the other polymers in the ground state and in excited states may be responsible for the remarkable differences in λ_{max} values.

Prior to CPL measurements, the polymer films were thermally annealed to increase anisotropy of the films. In the case of polyfluorenes with linear, chirality source groups, polymer films had to be thermally annealed to achieve high g_{CPL} values in CPL emission.⁶ Indeed, the polymers investigated in this work showed endothermic thermal transitions due to glass transition from differential scan calorimetry (DSC) analyses (Fig. S4). Thermal annealing was conducted at around the endothermic transition temperature to achieve ordered alignment of the polymer chains.

While CD spectra did not show a clear response to annealing the films of the homopolymer and the random copolymers (Fig. S5), CD intensity of the alternating copolymer film remarkably increased on heating at 160 °C and reached a constant value in 48 h (Fig. 3A). The g_{CD} value was as high as 0.026 at 393 nm. At the same time, hypochromism was observed in UV-vis spectra, and the intensity of the emission band in the range of 500–650 nm remarkably increased.

The emission band at around 550 nm could indicate either formation of inter-chain excimer or generation of 9-fluorenone

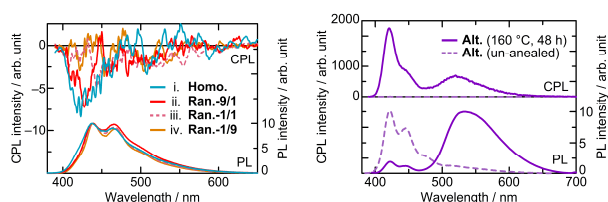


Fig. 4 CPL and fluorescence (PL) spectra of un-annealed film samples of the homopolymer and the random copolymers (left) and the thermally annealed and the un-annealed films of the alternating copolymer (right). λ_{ex} : in PL spectra, 366 nm for all the film samples; in CPL spectra, 350 nm for all the polymers.

Table 2 The ground-state and excited-state anisotropies.

Polymer	Un-annealed		Thermally annealed	
	$g_{\text{CD}} \times 10^4$	$g_{\text{CPL}} \times 10^4$	$g_{\text{CD}} \times 10^4$	$g_{\text{CPL}} \times 10^4$
Homo.	-1.1 (383 nm)	-5.9 (423 nm)	-1.0 (380 nm)	-3.3 (419 nm)
Ran.-9/1	-1.1 (381 nm)	-5.0 (427 nm)	-1.0 (381 nm)	-2.8 (424 nm)
Ran.-1/1	-0.5 (383 nm)	-3.5 (443 nm)	-0.7 (389 nm)	-3.8 (441 nm)
Ran.-1/9	-0.4 (381 nm)	-2.5 (453 nm)	-0.7 (358 nm)	-3.9 (452 nm)
Alt.	-0.2 (367 nm)	<0.5 (423 nm)	+260 (393 nm)	+1600, +250 (423, 520 nm)
NPF (in THF)	-3.5 (270 nm)	-6.0 (330 nm)	-	-

Thermal annealing conditions: temp. = 150 °C (**Homo.**), 140 °C (**Ran.-9/1**), 80 °C (**Ran.-1/1**), 60 °C (**Ran.-1/9**), and 160 °C (**Alt.**), time = 2 h (**Homo.** and **Ran.-9/1**, **-1/1**, **-1/9**), 48 h (**Alt.**), atmosphere = air, in the dark.

moiety (keto defect).²⁰ This aspect was assessed by redissolving the annealed polymer in THF and measuring UV and fluorescent spectra; however, the solution spectra did not indicate any clear evidence of keto defect (Fig. S7).²⁰ These results strongly suggest that the emission signal at around 550 nm is based mainly on intra-chain excimer formation that occurs only in the solid state. However, a very small increase in the intensity around 1700 cm^{-1} was detected in IR spectra of the annealed polymer (Fig. S6). Contributions from keto defect to the emission of **Alt.** in the solid state can not be completely ruled out through a comparison with the related literatures.²⁰

It is not yet clear at this point why only the alternating copolymer sharply responds to thermal annealing in film. Higher flexibility of **Alt.** chain might be responsible (see, Supplementary Information, p14). Evidently, the alternating monomeric sequence is very effective in making the main-chain twist bias larger on thermally aligning the chains. Importance of alternating sequences has been pointed out also for another other type of polymer.^{6f,g} Polarized optical microscopic observation on the alternating copolymer on heating suggested that the polymer tends to form ordered structure such as liquid crystals (Fig. S8).

Finally, CPL spectra of all polymers were measured (Fig. 4). For all polymers, polarization in emission was confirmed by the CPL spectra though $|g_{\text{CPL}}|$ values are rather small for the homopolymer and the random copolymers. In a sharp contrast, the alternating copolymer in the annealed film indicated much more intense CPL signals in a broad range from 400 nm through 650 nm compared with the other polymers. The anisotropy is larger by a degree of

magnitude than that of films of another alternating copolyfluorene reported by Meskers.^{6f}

Thickness of **Alt.** film was found to be around 0.33–1.31 μm . Hence, the intense CPL of the **Alt.** film may be contributed, to a certain extent, by the effect of film thickness proposed by Meskers.^{6d} It should be noted for this spectrum that CPL anisotropy is larger in the shorter-wavelength regions than in the range of 500–650 nm based on intermolecular excimer. This suggests that the large g_{CPL} value is mainly due to conformational anisotropy of single chain.

Table 2 summarizes g_{CD} and g_{CPL} values. It is noteworthy that the annealed alternating copolymer film exceptionally provides the greatest $|g_{\text{CPL}}|$ value of -0.16 at 420 nm, corresponding to 8 % of the ideal circular polarization where $|g_{\text{CPL}}|$ is 2. This $|g_{\text{CPL}}|$ value is much greater than the corresponding $|g_{\text{CD}}|$ value of the same film by almost one order of magnitude. This chirality amplification in excited states may arise from a conformational transition of the main chain leading to a higher twist bias. Probably, free energy potential of the chain in the photoexcited states significantly differs from that in the ground state. This aspect needs to be further clarified by a theoretical point of view. Chirality amplification in excited states seems to take place also for most of the polymers studied here. This is in a sharp contrast to previously reported linear, chiral polymer emitter systems.²¹

In addition, the $|g_{\text{CD}}|$ and $|g_{\text{CPL}}|$ values of the alternating copolymer film are enhanced, respectively, by three and four orders of magnitude by thermal annealing. This means that thermal annealing effectively induces a conformational transition leading to amplification of chirality in the ground state.

Conclusions

In conclusion, we synthesized novel, optically active polyfluorene derivatives bearing neomenthyl group in the side chain as chirality source. Among the polymers, the alternating copolymer indicated a remarkable enhancement of chirality in the ground state on annealing, and it showed an exceptionally highly efficient CPL emission. Also, for most of the polymers studied in this work, g_{CPL} (excited-state chirality) was greater than g_{CD} (ground-state chirality). This is the first clear demonstration of amplification of polymer chirality in the photoexcited states for linear polymer systems.

In a recent study, a chiral fluorene-thiophene copolymer indicated a $|g_{\text{CD}}|$ of 0.3 while $|g_{\text{CPL}}|$ was 0.2.⁶ⁱ Also, bimolecular systems consisting of achiral polymer and chiral dopant a $|g_{\text{CD}}|$ of 0.2 for $|g_{\text{CPL}}| = 0.5$ ^{21a} and a $|g_{\text{CD}}|$ of 0.1 for a $|g_{\text{CPL}}|$ of 0.08.^{21b} Chirality amplification by almost one order of magnitude of g value in excited states reported here is still rare.

Also, importance of LC order and film thickness effects on chiral emission of polymers have been found and studied by Meskers.^{6d-h} These features may have significant influences on the properties of the polymers synthesized in this study and will be assessed in our future work.^{6d-h}

Acknowledgements

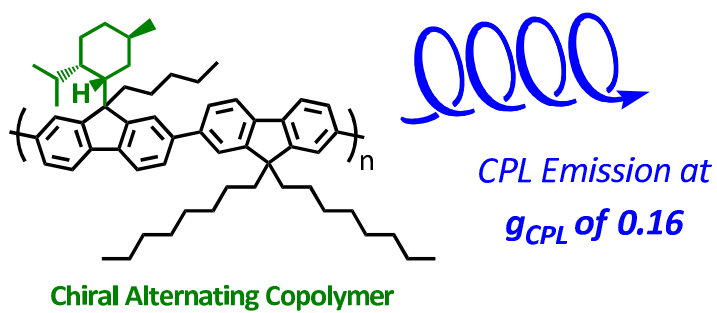
This study was funded in part by Catalysis Research Center (CRC), in part by the Sumitomo Foundation, in part by the Asahi Glass Foundation, and in part by JSPS Research Fellowships for Young

Scientists for K.W. (No. 25-2727) by the Japan Society for the Promotion of Science.

Notes and references

- 1 a) M. T. Bernius, M. Inbasekaran, J. O'Brien and W. S. Wu, *Adv. Mater.*, 2000, **12**, 1737; b) D. Neher, *Macromol. Rapid Commun.*, 2001, **22**, 1365; c) U. Scherf and E. J. W. List, *Adv. Mater.*, 2002, **14**, 477.
- 2 a) M. Suarez and G. B. Schuster, *J. Am. Chem. Soc.*, 1995, **117**, 6732; b) Y. F. Zhang and G. B. Schuster, *J. Org. Chem.*, 1995, **60**, 7192; c) N. P. M. Huck, W. F. Jager, B. de Lange and B. L. Feringa, *Science*, 1996, **273**, 1686; d) T. K. Lim, S. U. Choi, S. D. Lee and Y. I. Park, *Jpn. J. Appl. Phys.*, 1996, **35**, L1281; e) C. S. Wang, H. S. Fei, Y. Qui, Y. Q. Yang, Z. Q. Wei, Y. Q. Tian, Y. M. Chen and Y. Y. Zhao, *Appl. Phys. Lett.*, 1999, **74**, 19.
- 3 M. Schadt, *Annu. Rev. Mater. Sci.*, 1997, **27**, 305.
- 4 D. J. Broer, J. Lub and G. N. Mol, *Nature*, 1995, **378**, 467.
- 5 a) E. Peeters, M. P. T. Christiaans, R. A. J. Janssen, H. F. M. Schoo, H. P. J. M. Dekkers and E. W. Meijer, *J. Am. Chem. Soc.*, 1997, **119**, 9909; b) A. Satrijo, S. C. J. Meskers and T. M. Swager, *J. Am. Chem. Soc.*, 2006, **128**, 9030.
- 6 a) M. Oda, H.-G. Nothofer, G. Lieser, U. Scherf, S. C. J. Meskers, and D. Neher, *Adv. Mater.*, 2000, **12**, 362; b) M. Oda, H.-G. Nothofer, U. Scherf, V. Šunjić, D. Richter, W. Regenstein, and D. Neher, *Macromolecules*, 2002, **35**, 6792; c) X. H. Yang, D. Neher, C. Spitz, E. Zojer, J. L. Brédas, R. Güntner, and U. Scherf, *J. Chem. Phys.*, 2003, **119**, 6832; d) M. R. Craig, P. Jonkheijm, S. C. J. Meskers, A. P. H. J. Schenning, and E. W. Meijer, *Adv. Mater.*, 2003, **15**, 1435; e) R. Abbel, A. P. H. J. Schenning, and E. W. Meijer, *Macromolecules*, 2008, **41**, 7497; f) J. Gilot, R. Abbel, G. Lakhwani, E. W. Meijer, A. P. H. J. Schenning and S. C. J. Meskers, *Adv. Mater.*, 2010, **22**, E131; g) G. Lakhwani and S. C. J. Meskers, *J. Phys. Chem. Lett.*, 2011, **2**, 1497; h) G. Lakhwani and S. C. J. Meskers, *J. Phys. Chem. A*, 2012, **116**, 1121; i) T. Hirahara, M. Yoshizawa-Fujita, Y. Takeoka and M. Rikukawa, *Chem. Lett.*, 2012, **41**, 905.
- 7 a) J. N. Wilson, W. Steffen, T. G. McKenzie, G. Lieser, M. Oda, D. Neher and U. H. F. Bunz, *J. Am. Chem. Soc.*, 2002, **124**, 6830; b) A. Satrijo, S. C. J. Meskers and T. M. Swager, *J. Am. Chem. Soc.*, 2006, **128**, 9030.
- 8 a) S. Fukano and M. Fujiki, *Macromolecules*, 2009, **42**, 8062; b) Y. Nakano, F. Ichianagi, M. Naito, Y. G. Yang and M. Fujiki, *Chem. Commun.*, 2012, **48**, 6636.
- 9 B. M. W. L.-Voss, R. A. J. Janssen, M. P. T. Christiaans, S. C. J. Meskers, H. P. J. M. Dekkers and E. W. Meijer, *J. Am. Chem. Soc.*, 1996, **118**, 49089.
- 10 J.-M. Yu, T. Sakamoto, K. Watanabe, S. Furumi, N. Tamaoki, Y. Chen and T. Nakano, *Chem. Commun.*, 2011, **47**, 3799.
- 11 K. Watanabe, T. Sakamoto, M. Taguchi, M. Fujiki and T. Nakano, *Chem. Commun.*, 2011, **47**, 10996.
- 12 Y. Morisaki, R. Hifumi, L. Lin, K. Inoshita and Y. Chujo, *Polym. Chem.*, 2012, **3**, 2727.
- 13 R. Noyori, *Angew. Chem., Int. Ed.*, 2002, **41**, 2008.
- 14 A. Gutnov, H.-J. Drexler, A. Spannenberg, G. Oehme and B. Heller, *Organometallics*, 2004, **23**, 1002.
- 15 K. Tamao, K. Sumitani and M. Kumada, *J. Am. Chem. Soc.*, 1972, **94**, 4374.
- 16 a) N. Miyaura, K. Yamada and A. Suzuki, *Tetrahedron Lett.*, 1979, **20**, 3437; b) N. Miyaura and A. Suzuki, *J. Chem. Soc. Chem. Commun.*, 1979, **866**; c) N. Miyaura and A. Suzuki, *Chem. Rev.*, 1995, **95**, 2457.
- 17 a) M. A. Haney, C. Jackson and W. W. Yau, *Water's International GPC Symposium Proceedings*, Oct. 14–16, 1991, 49; b) A. Striegel, W. W. Yau, J. J. Kirkland and D. D. Bly, *Modern Size Exclusion Liquid Chromatography*, Wiley, New York, 1979; c) S. E. Harding, *Prog. Biophys. Mol. Biol.*, 1997, **68**, 207; d) H. L. Wagner, *J. Phys. Chem. Ref. Data*, 1985, **14**, 1101.
- 18 Y. Wang, T. Sakamoto and T. Nakano, *Chem. Commun.*, 2012, **48**, 1871.
- 19 H. Kameshima, N. Nemoto and T. Endo, *J. Polym. Sci., Part A: Polym. Chem.*, 2001, **39**, 3143.
- 20 a) E. J. W. List, R. Guentner, P. Scanducci de Freitas and U. Scherf, *Adv. Mater.*, 2002, **14**, 374; b) C. Chi, C. Im, V. Enkelmann, A. Ziegler, G. Lieser and G. Wegner, *Chem. Eur. J.*, 2005, **11**, 6833; c) J.-R. Wu, Y. Chen and T.-Y. Wu, *J. Appl. Poly. Sci.*, 2011, **119**, 2576; d) S. J. Hintschich, C. Rothe, S. Sinha, A. P. Monkman, P. Scanducci de Freitas and U. Scherf, *J. Chem. Phys.*, 2003, **119**, 12017.
- 21 a) Y. Yang, R. Correa da Costa, D.-M. Smilgies, A. J. Campbell and M. J. Fuchter, *Adv. Mater.*, 2013, **25**, 2624; b) M. Fujiki, A. J. Jalilah, N. Suzuki, M. Taguchi, W. Zhang, M. M. Abdellatif and K. Nomura, *RSC Adv.*, 2012, **2**, 6663.

For graphical abstract



Anisotropy of an alternating copolyfluorene consisting of chiral and achiral units is remarkably amplified in the ground and excited states.

Supplementary Information for:

Gigantic Chiroptical Enhancements in Polyfluorene Copolymers Bearing Bulky Neomenthyl Group: Importance of Alternating Sequence of Chiral and Achiral Fluorene Units

Kento Watanabe,^[a] Yasuhito Koyama,^[a] Nozomu Suzuki,^[b] Michiya Fujiki,^[b] and Tamaki Nakano*^[a]

^aCatalysis Research Center and Graduate School of Chemical Sciences and Engineering, Hokkaido University, Sapporo 001-0021, Japan [E-mail: tamaki.nakano@cat.hokudai.ac.jp]

^bGraduate School of Materials Science, Nara Institute of Science and Technology, Takayama-cho 8916-5, Nara 630-0101, Japan

General Methods:

Materials. Tetrahydrofuran (THF) (Wako Pure Chemical) was dried on sodium benzophenone ketyl and distilled immediately before use. The other chemicals listed as follows were used without purification: *l*-menthol, pyridine, chloroform, *n*-butyllithium (1.57 M in *n*-hexane solution) 1-iodopentane, bromine, iodine, dichloromethane, dimethyl sulfoxide, magnesium (turnings), 1,2-dibromoethane, and potassium carbonate (Kanto Chemical); 1,4-dioxane (Nacalai Tesque); triphenylphosphine, and *p*-toluenesulfonyl chloride (Wako Pure Chemical Industries, Ltd.); fluorene, hydrazine monohydrate, and dichloro[1,3-bis(diphenylphosphino)propane]nickel(II) (Tokyo Chemical Industry); palladium(II) chloride, 2,7-dibromo-9,9-dioctylfluorene, and 9,9-dioctylfluorene-2,7-diboronic acid bis(1,3-propanediol) ester) (Sigma-Aldrich).

Measurements. ¹H NMR spectra were recorded on a JEOL JNM-ESC400 spectrometer (400 MHz for ¹H). SEC was carried out using a chromatographic system consisting of a Hitachi L-7100 chromatographic pump, a Hitachi L-7420 UV detector (254 nm), and a Hitachi L-7490 RI detector equipped with TOSOH TSK gel G3000H HR and G6000H HR columns (30 x 0.72 (i.d.) cm) connected in series (eluent THF, flow rate 1.0 mL/min). SEC was also performed using Wyatt Technology Dawn EOS-N MALLS detector and Viscotek Model TDA300 on-line RI and viscometric detectors. Right-angle scattering information was obtained from the MALLS detector and integrated into the TDA detector system to calculate molar masses and Mark-Houwink-Sakurada constants. Absorption spectra were measured at room temperature with a JASCO V-570 spectrophotometer. CD and LD spectra were taken on a JASCO J-820 spectrometer. Fluorescent spectra were taken on a JASCO FP-8500 fluorescence spectrophotometer. Absolute fluorescence quantum yield was determined with a JASCO FP-8500 fluorescence spectrophotometer attached with an ILF-835 100-mm ϕ integral sphere unit. FT-IR spectra were measured using a Thermo

Fischer Scientific Nexus 870 spectrometer. Optical rotation was measured with a JASCO P-1030 digital polarimeter. DSC analyses were performed on Rigaku Thermo plus TG8120 and DSC8230 apparatuses using Thermo plus 2 software for data analyses. Polarized optical microscopic observations were conducted using a Nikon Eclipse E600 POL microscope. CPL-fluorescent spectra were taken on a JASCO CPL-200 (NAIST, Japan). X-ray diffraction (XRD) profiles were obtained using a Rigaku Miniflex diffractometer.

Film fabrication. Polymer films were fabricated by drop-casting a CHCl_3 solution (8 mg/mL, 20 μL) onto a quartz plate (size: 1 cm \times 2 cm, thickness: 1 mm). The film thickness was in a range from ca. 0.33 to 1.31 μm , which was taken on a Keyence laser scanning microscope VK 9700.

Monomer synthesis:

Menthyltosylate. This compound was synthesized according to the literature [G. Erker, M. Aulbach, M. Knickmeier, D. Wingbermhühle, C. Krüger, M. Nolte, S. Werner, *J. Am. Chem. Soc.* **1993**, *115*, 4590–4601] with modifications.

p-Toluenesulfonyl chloride (26.6 g, 0.14 mol) dissolved in 60 mL of CHCl_3 was slowly added to a solution of *l*-menthol (20.0 g, 0.13 mol) in 41 mL of pyridine cooled at 0 °C. The reaction mixture was stirred at room temperature for 3 h. Removal of solvents gave a crude product. The crude material was dissolved in MeOH, and water was slowly added to the solution. This process yielded colorless crystals (m.p. 89 °C). Yield: 34.2 g (87%).

9-Neomenthylfluorene. This compound was synthesized according to the literature [A. Gutnov, H.-J. Drexler, A. Spannenberg, G. Oehme, and B. Heller, *Organometallics*, **2004**, *23*, 1002–1009] with modifications.

To a solution of fluorene (26.1 g, 0.16 mol) in 120 mL of THF cooled at 0 °C was slowly added 100 mL (0.16 mol) of *n*-BuLi (1.57 M in *n*-hexane solution). The reaction mixture was stirred for 30 min at 0 °C. After the reaction system was cooled to –78 °C, menthyltosylate (24.0 g, 0.08 mol) dissolved in 120 mL of THF was added in several portions. The reaction mixture was stirred at room temperature for 30 min and for additional 15 h under reflux, and then was poured into a large excess of iced water. The crude product was extracted with CHCl_3 , and the organic layer was dried on MgSO_4 . The crude material was first purified by silica-gel column chromatography with a mixture of toluene and *n*-hexane (1/10, v/v) as eluent and was then recrystallized from methanol to afford colorless crystals (m.p. 63–65 °C). Yield: 5.3 g (22%).

9-Neomenthyl-9-*n*-pentylfluorene. This compound was synthesized by the method of the literature [J.-M. Yu, T. Sakamoto, K. Watanabe, S. Furumi, N. Tamaoki, Y. Chen, and T. Nakano, *Chem. Commun.*, **2011**, *47*, 3799–3801].

To a solution of 9-neomenthylfluorene (4.0 g, 13.2 mol) in 70 mL of THF cooled at 0 °C was slowly

added 10.0 mL (15.7 mol) of *n*-BuLi (1.57 M in *n*-hexane solution). After the reaction system was stirred at 0 °C for 1 h, 1-iodopentane (3.9 g, 19.7 mol) dissolved in 10 mL of THF was slowly added. The resulting mixture was warmed to room temperature, was stirred for 24 h, and was poured into a large excess of iced water. The crude product was extracted with CHCl₃, and the organic layer was dried on MgSO₄. The crude material was purified by silica-gel column chromatography with a mixture of toluene and *n*-hexane (1/5, v/v) as eluent to afford a colorless oily product. Yield: 4.6 g (92%); [α]_D²⁵ -51 (c. 1.00, CHCl₃).

2,7-Dibromo-9-neomenthyl-9-*n*-pentylfluorene (DBNPF). This compound was synthesized according to the literature [R. Kannan, B. A. Reinhardt, and L.-S. Tan, U.S. Patent, 6,300,5, Oct 9, 2001] with modifications.

To a solution of NPF (10.3 g, 27.4 mmol) and iodine (83.5 mg, 0.3 mmol) in 52 mL of CH₂Cl₂ was added dropwise bromine (3.0 mL, 58.6 mmol). After the reaction system was stirred at room temperature for 1.5 h, it was poured into an excess of aq. NaHSO₃. The crude product was extracted with CH₂Cl₂. The organic layer was washed with brine and was dried on MgSO₄. The crude product was purified by recrystallization with *n*-hexane to afford colorless crystals (m.p. 145 °C). Yield: 12.4 g (85%); [α]_D²⁶ +9.0 (c. 1.00, CHCl₃).

Polymerization

Tetrakis(triphenylphosphine)palladium(0) (Pd(PPh₃)₄). This compound was synthesized according to the literature [D. R. Coulson, *Inorg. Synth.*, **1972**, *13*, 121–124; *ibid.*, **1990**, *28*, 107–109].

In a two-necked flask, PdCl₂ (1.5 g, 8.5 mmol) and triphenylphosphine (11.1 g, 42.3 mmol) were dissolved in 105 mL of dimethyl sulfoxide (DMSO). After the reaction mixture was stirred at 150 °C for 15 min, hydrazine monohydrate (1.7 mL, 33.9 mmol) was added dropwise to the system. The reaction system was then cooled to room temperature. The product was separated from the reaction mixture as yellow powder by filtration and was washed with EtOH and Et₂O in this order. Yield: 9.1 g (93%).

Random Copolymerization of DBNPF with 2,7-Dibromo-9,9-dioctylfluorene (DBDOF) and Homopolymerization of DBNPF. In a Schlenk tube, magnesium (turnings, 70 mg, 2.9 mmol) was activated with 1,2-dibromoethane (188 mg, 1.0 mmol) in 1 mL of THF. For a random copolymerization, prescribed amounts of DBNPF and DBDOF dissolved in 3 mL of THF was added in several portions to activated magnesium, and the mixture was stirred at 60 °C for 1 h (see Table S1 for the amounts of the monomers). Ni(dppp)Cl₂ (20.4 mg, 0.04 mmol) was added to the system, the mixture was stirred at 60 °C for 24 h, and the reaction was quenched by adding 7 mL of 0.1 M aq.

HCl. The crude product was extracted with CHCl_3 , and the organic layer was dried on MgSO_4 . Removal of CHCl_3 afforded the crude polymer as yellow, crude powder. The crude material was dissolved in 20 mL of CHCl_3 , and the solution was poured into 600 mL of MeOH. The precipitates were collected with a centrifuge. Homopolymerization was conducted in the same manner as random copolymerization. Amounts of monomers used for reactions are shown in Table S1.

Table S1. Amounts of monomers used for random copolymerization and homopolymerization.

Entry	Polymerization Type	DBNPF		DBDOF		Molar Ratio	Obtained Polymer
		Amount	Molar	Amount	Molar		
1	Homopolymerization	1.00 g	1.90 mmol	-	-	1/0	Homo.
2	Random copolymerization	0.90 g	1.71 mmol	0.10 g	0.19 mmol	9/1	Ran.-9/1
3	Random copolymerization	0.50 g	0.95 mmol	0.52 g	0.95 mmol	1/1	Ran.-1/1
4	Random copolymerization	0.10 g	0.19 mmol	0.93 g	1.71 mmol	1/9	Ran.-1/9

Homo.: 77% yield; $[\alpha]_D^{25}$ -0.5 (c. 4.00, THF); M_n 11,800 (estimated by SEC on the basis of polystyrene standards); M_w/M_n 4.15 (estimated by SEC on the basis of polystyrene standards); M_n 10,400 (determined by SEC-VISC-RALS); M_w/M_n 1.56 (determined by SEC-VISC-RALS); T_g 127 °C; T_d 314 °C; $^1\text{H NMR}$ (400 MHz, CDCl_3 , 293 K) δ 7.83–7.31 (m), 2.77 (brd), 2.66 (brd), 2.24 (brd), 2.06 (brd), 1.75 (brd), 1.54 (brd), 1.36 (brd), 1.18 (brd), 1.15 (brd), 1.13 (brd), 0.87 (brd), 0.83 (brd), 0.73 (brd), 0.72 (brd), 0.68 (brd), 0.59 (brd), 0.52 (brd), 0.50 (brd), 0.28 (brd), 0.24 (brd), 0.21 (brd), 0.16 (brd) ppm; IR (KBr) ν 2954, 2927, 2861, 1608, 1457, 1377, 1260, 1095, 1022, 888, 811, 743 cm^{-1} .

Ran.-9/1: 72% yield; $[\alpha]_D^{25}$ -0.6 (c. 4.00, THF); M_n 19,500 (estimated by SEC on the basis of polystyrene standards); M_w/M_n 3.45 (estimated by SEC on the basis of polystyrene standards); M_n 10,000 (determined by SEC-VISC-RALS); M_w/M_n 1.57 (determined by SEC-VISC-RALS); T_g 120 °C; T_d 298 °C; $^1\text{H NMR}$ (400 MHz, CDCl_3 , 293 K) δ 7.83–7.31 (m), 2.77 (brd), 2.66 (brd), 2.24 (brd), 2.06 (brd), 1.76 (brd), 1.54 (brd), 1.24 (brd), 1.18 (brd), 1.13 (brd), 0.81 (brd), 0.73 (brd), 0.69 (brd), 0.68 (brd), 0.59 (brd), 0.52 (brd), 0.50 (brd), 0.28 (brd), 0.24 (brd), 0.16 (brd) ppm; IR (KBr) ν 2954, 2929, 2864, 1609, 1459, 1379, 1260, 1095, 1018, 889, 814, 742 cm^{-1} .

Ran.-1/1: 84% yield; $[\alpha]_D^{25}$ $+0.6$ (c. 4.00, THF); M_n 13,400 (estimated by SEC on the basis of polystyrene standards); M_w/M_n 4.17 (estimated by SEC on the basis of polystyrene standards); M_n 8,800 (determined by SEC-VISC-RALS); M_w/M_n 1.70 (determined by SEC-VISC-RALS); T_g 67 °C;

T_d 297 °C; $^1\text{H NMR}$ (400 MHz, CDCl_3 , 293 K) δ 7.82–7.32 (m), 2.75 (brd), 2.65 (brd), 2.25 (brd), 2.10 (brd), 1.76 (brd), 1.55 (brd), 1.24 (brd), 1.13 (brd), 0.87 (brd) 0.81 (brd), 0.79 (brd), 0.72 (brd), 0.71 (brd), 0.59 (brd), 0.52 (brd), 0.28 (brd), 0.21 (brd) 0.15 (brd) ppm; IR (KBr) ν 2937, 2927, 2855, 1609, 1459, 1404, 1377, 1259, 1096, 1024, 887, 814, 743 cm^{-1} .

Ran.-1/9: 84% yield; $[\alpha]_D^{25}$ +0.3 (c. 4.00, THF); M_n 18,400 (estimated by SEC on the basis of polystyrene standards); M_w/M_n 5.11 (estimated by SEC on the basis of polystyrene standards); M_n 16,400 (determined by SEC-VISC-RALS); M_w/M_n 1.82 (determined by SEC-VISC-RALS); T_g 32 °C; T_d 301 °C; $^1\text{H NMR}$ (400 MHz, CDCl_3 , 293 K) δ 7.84–7.28 (m), 2.75 (brd), 2.11 (brd), 2.03 (brd), 1.76 (brd), 1.55 (brd), 1.26 (brd), 1.24 (brd), 1.13 (brd), 0.81 (brd), 0.72 (brd), 0.59 (brd), 0.52 (brd), 0.27 (brd), 0.21 (brd), 0.15 (brd) ppm; IR (KBr) ν 2926, 2853, 1610, 1459, 1405, 1375, 1259, 1096, 1024, 886, 814, 742 cm^{-1} .

Alternating copolymerization of DBNPF with 9,9-dioctylfluoren-2,7-diboronic acid bis(1,3-propanediol) ester. In a flask equipped with a reflux condenser, **DBNPF** (240 mg, 0.45 mmol) and 2,7-di(1,3,2-dioxaborolan-2-yl)-9,9-di-*n*-octylfluorene (250 mg, 0.45 mmol) were dissolved in 4 mL of 1,4-dioxane. $\text{Pd}(\text{PPh}_3)_4$ (52 mg, 0.05 mmol), K_2CO_3 (0.43 g, 3.08 mmol), and 1.5 mL of water were added to the flask. After the reaction mixture was stirred at 110 °C for 2.5 h, 7 mL of 0.1 M aq. HCl was added to the system. The crude product was extracted with CHCl_3 , and the organic layer was dried on MgSO_4 . Removal of CHCl_3 afforded the crude material as yellow solid. The crude material was dissolved in 20 mL of CHCl_3 , and the solution was poured into 600 mL of MeOH. The precipitates were collected with a centrifuge to give **Alt.**; 72% yield; $[\alpha]_D^{25}$ +0.9 (c. 4.00, THF); M_n 25,300 (estimated by SEC on the basis of polystyrene standards); M_w/M_n 5.27 (estimated by SEC on the basis of polystyrene standards); M_n 22,300 (determined by SEC-VISC-RALS); M_w/M_n 2.35 (determined by SEC-VISC-RALS); T_g 85 °C; T_d 304 °C; $^1\text{H NMR}$ (400 MHz, CDCl_3 , 293 K) δ 7.83–7.31 (m), 2.77 (brd) 2.25 (brd), 2.10 (brd), 1.78 (brd), 1.56 (brd), 1.13 (brd), 0.87 (brd), 0.80 (brd), 0.72 (brd), 0.59 (brd), 0.50 (brd), 0.26 (brd), 0.20 (brd) ppm; IR (KBr) ν 2927, 2855, 1608, 1458, 1403, 1378, 1256, 1115, 889, 814, 750, 727, 696 cm^{-1} .

Supporting Figures and Tables

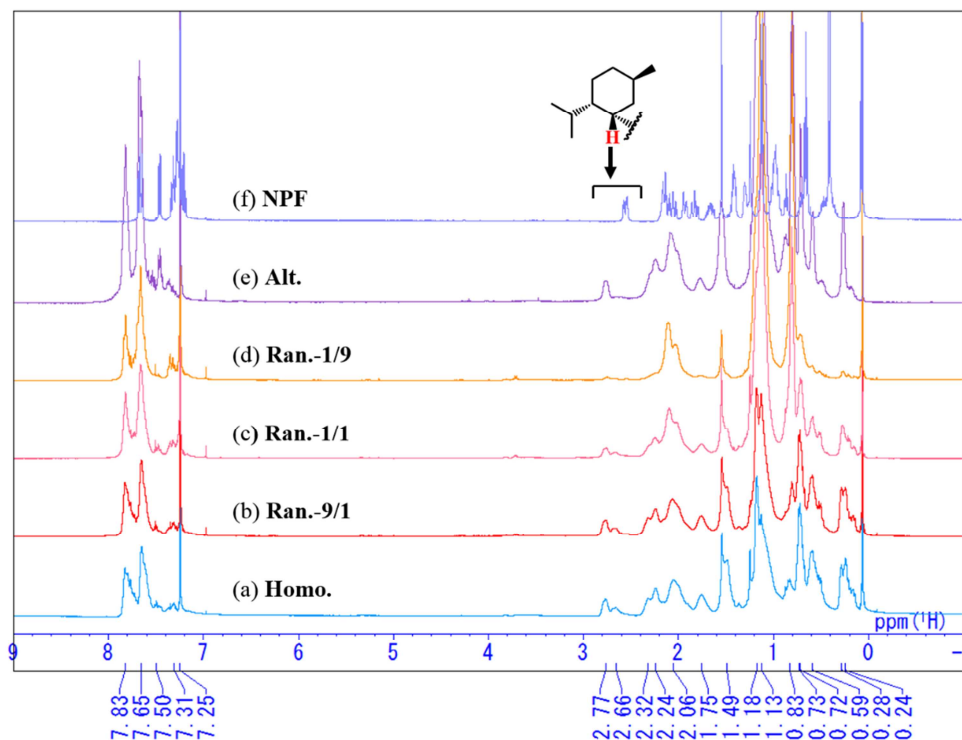


Figure S1. ^1H NMR spectra of the polymers and NPF; **Homo.** (a), **Ran.-9/1** (b), **Ran.-1/1** (b), **Ran.-1/9** (d), **Alt.** (e), and **NPF** (f). [400 MHz, CDCl_3 , r.t.]

Note: The peaks at around 2.5–2.8 ppm indicate the methine proton of neomenthyl moiety. While the peak in the spectrum (e, **Alt.**) appears as a unimodal peak, the peaks in the spectra of (a)-(c) of **Homo.**, **Ran.-1/1**, and **Ran.-1/9** appear as bimodal peaks attributed to the polymer tacticity. These results imply that the asymmetric field of the chiral repeating unit on **Alt.** would hardly reach the neighboring chiral units.

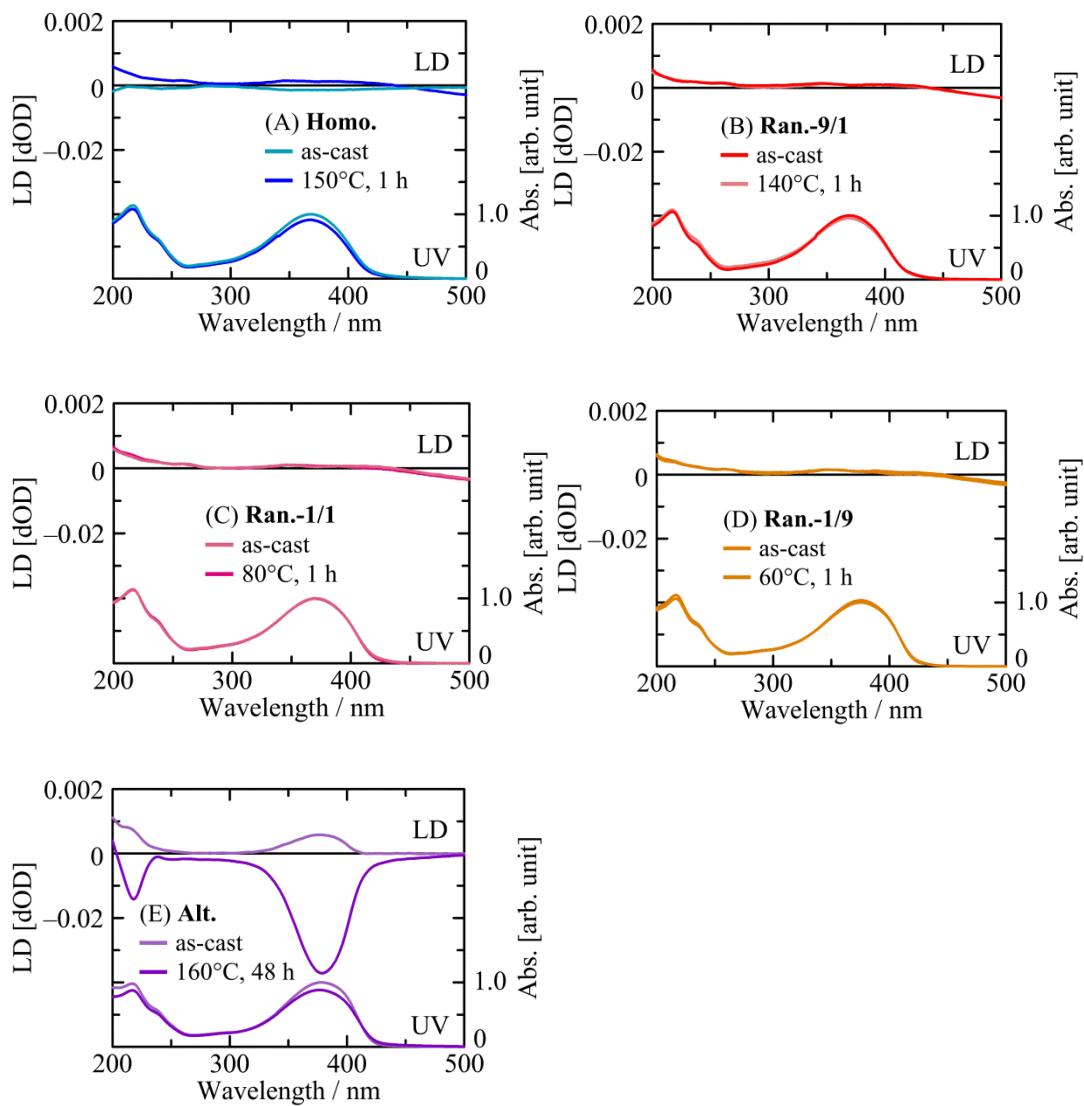


Figure S2. Linear dichroism (LD) and UV spectra of the polymers in film before and after thermal annealing; **Homo.** (A), **Ran.-9/1** (B), **Ran.-1/1** (C), **Ran.-1/9** (D), and **Alt.** (E).

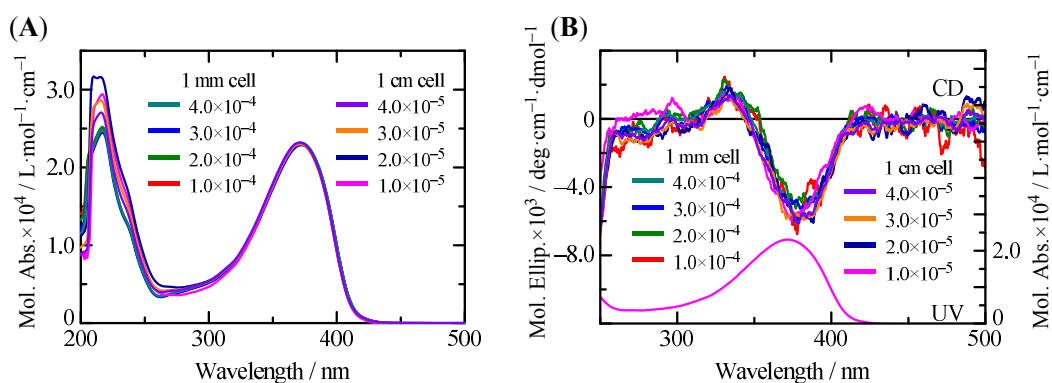


Figure S3. UV spectra (A) and CD spectra with a representative UV spectrum (B) spectra of the alternating copolymer measured at 1.0×10^{-5} M, 2.0×10^{-5} M, 3.0×10^{-5} M, 4.0×10^{-5} M, 1.0×10^{-4} M, 2.0×10^{-4} M, 3.0×10^{-4} M, and 4.0×10^{-4} M in THF.

Note: Chain aggregation in THF affecting polymer chirality is ruled out by these spectra. The spectra taken in the concentration range of 1×10^{-5} M to 4×10^{-4} M (per residue) did not show any significant differences.

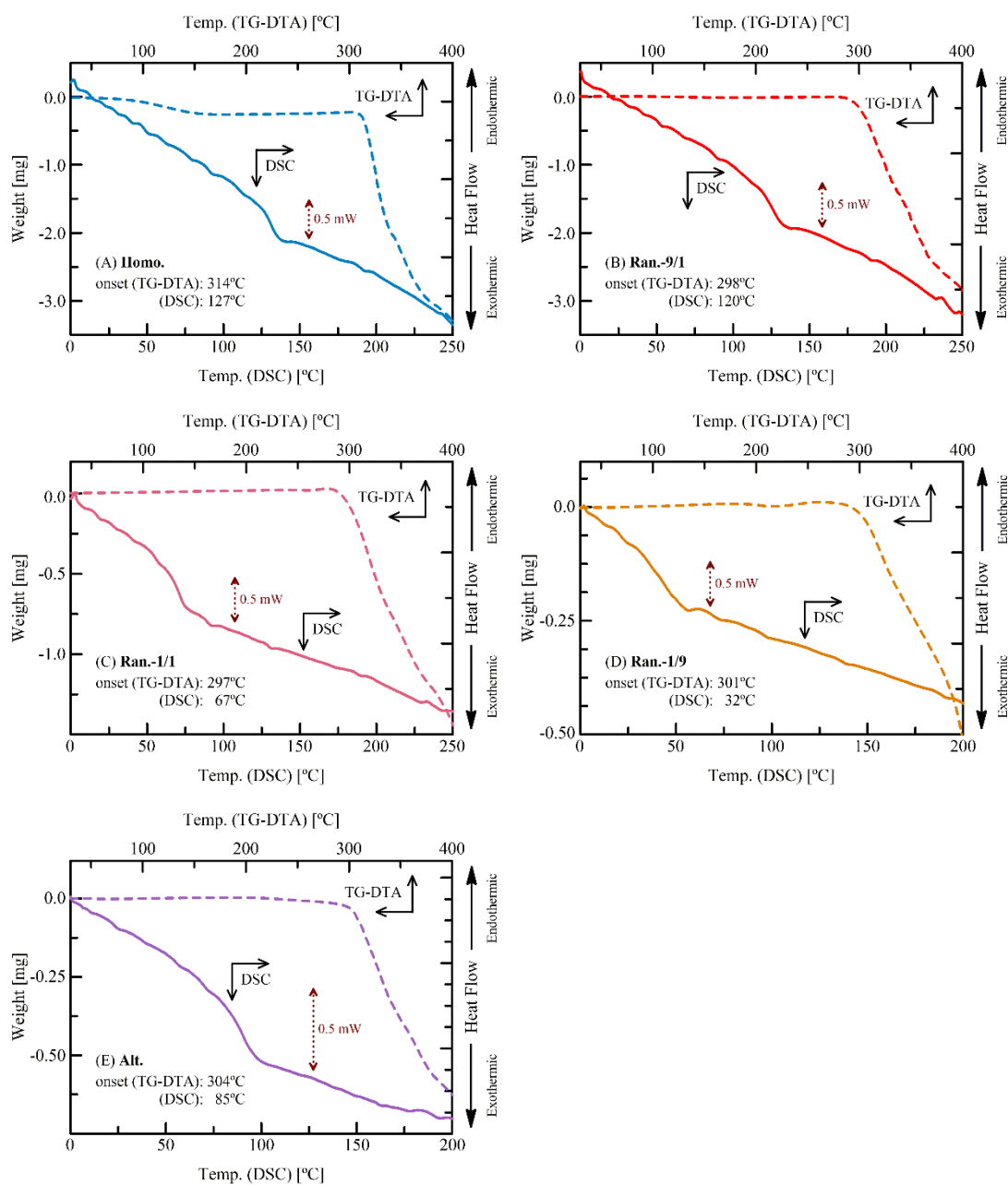


Figure S4. TG-DTA and DSC profiles of the polymers recorded under N_2 atmosphere; **Homo.** (A), **Ran.-9/1** (B), **Ran.-1/1** (C), **Ran.-1/9** (D), and **Alt.** (E). [sample weight for TD-TGA; 8.8 mg (A), 8.2 mg (B), 7.1 mg (C), 7.3 mg (D), and 3.2 mg (E): sample weight for DSC; 10.7 mg (A), 9.3 mg (B), 10.2 mg (C), 11.7 mg (D), and 8.1 mg (E)].

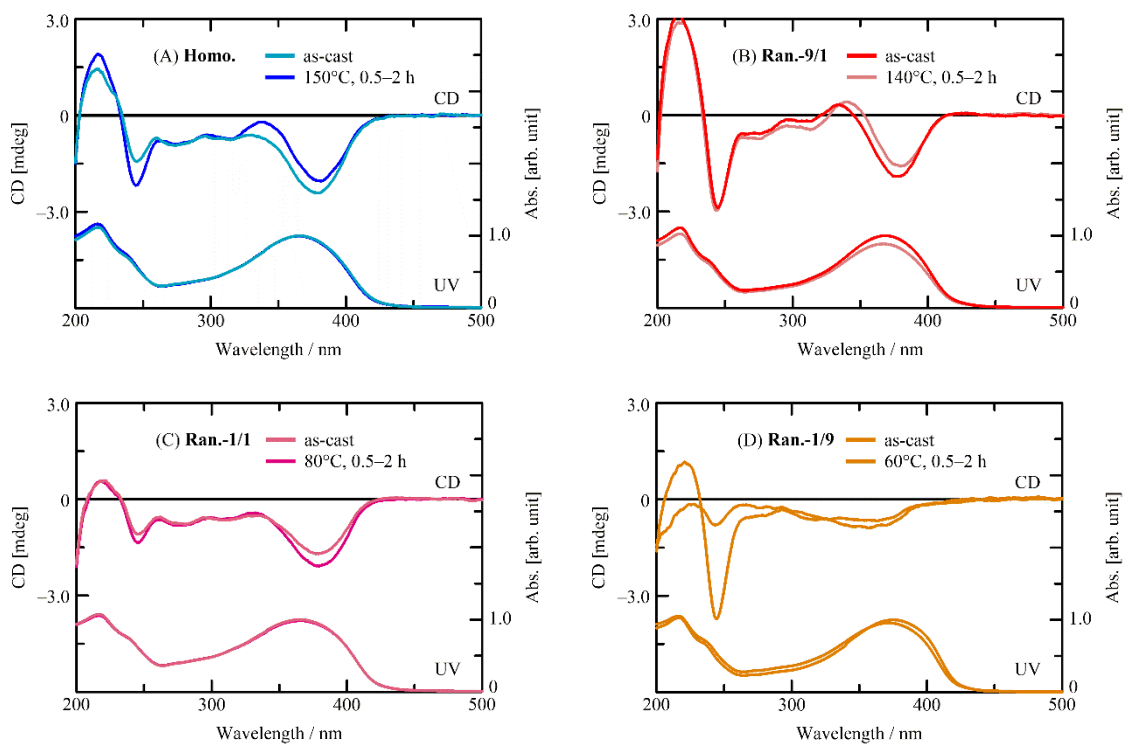


Figure S5. Changes in UV and CD spectra of the homopolymer and the random copolymer in film via thermal annealing; **Homo.** (A), **Ran.-9/1** (B), **Ran.-1/1** (C), and **Ran.-1/9** (D). [annealing temp. = 150 °C (A), 140 °C (B), 80 °C (C), and 60 °C (D); time* = 0.5 h, 1 h, and 2 h (A–D)] *On thermal annealing at the prescribed temperatures for 0.5 h, spectral changes were observed. However, on further heating for 1 h and 2 h, no changes were confirmed.

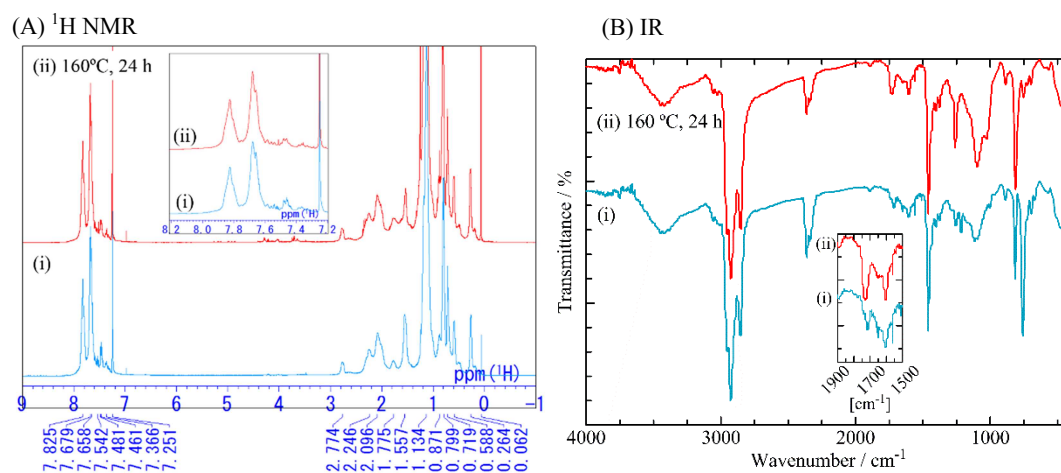


Figure S6. ^1H NMR (left) and IR (right) spectra of **Alt.** before (i) and after being annealed (ii). [(thermal annealing) in a film state on a glass plate, 160 °C, 24 h, under air, in the dark; (NMR) in CDCl_3 , 400 MHz, r.t.; (IR) KBr pellet, r.t.]

Note: According to ref. 20b, keto defect (fluoren-9-one moiety) in a poly(fluoren-2,7-diyl) derivative shows characteristic peaks at around 7.9 ppm in ^1H NMR spectra that were assigned to the protons on the 1- and 8-positions of the fluoren-9-one ring. The spectrum, (A)-(ii) showed no clear such peaks ruling out the possibility of keto defect generation. This conclusion is supported by IR spectra, (B)-(i) and (B)-(ii), showing no significant changes on annealing at around 1500-1900 cm^{-1} where an intense ketone $\text{C}=\text{O}$ stretching band could appear. Thus, the chemical structure of the alternating copolymer in film was not changed by thermal annealing.

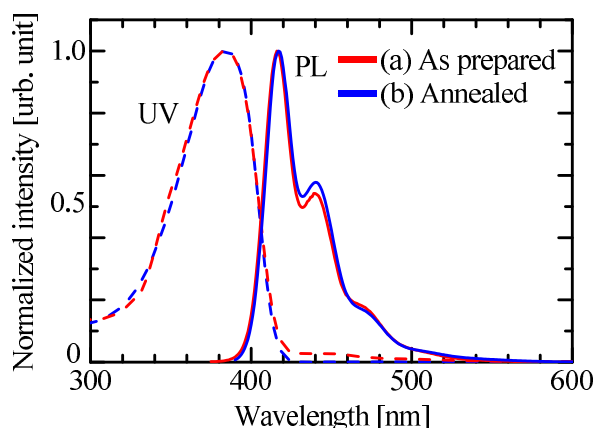


Figure S7. UV and PL spectra of the alternating copolymer in a THF solution; (a) as prepared and (b) after being annealed on a film.

Note: According to ref. 20c, an emission band at around 550 nm due to keto defect (fluorene-9-one moiety) was observed in solution for a poly(9,9-di-*n*-octylfluorene-2,7-diyl) where, for a polymer containing 33% of keto defect, the ratio of emission intensities of di-*n*-octylfluorene unit to fluorenone unit was 1/9.5. In addition, according to ref. 20d, for poly[9,9-bis(3,7,11-trimethyldodecyl)fluorene-2,7-diyl] containing only 1% of keto defect, the ratio of emission intensities of bis(3,7,11-trimethyldodecyl)fluorene unit to fluorenone unit was 1/6.2. These ratios were estimated by us using relevant figures in the references. Hence, the emission at around 550 nm is a very sensitive probe of keto defect. However, when the annealed alternating copolymer in film was re-dissolved in THF, it did not indicate the signal at around 550 nm in fluorescence due to ketone units at all (Figure S3), strongly supporting that the spectroscopic features observed for the alternating copolymer in this work is not based on keto defect. The emission band of the alternating copolymer at around 550 nm is observed only in film. This means that the band is due to inter-chain excimer formation that occurred only in the solid state.

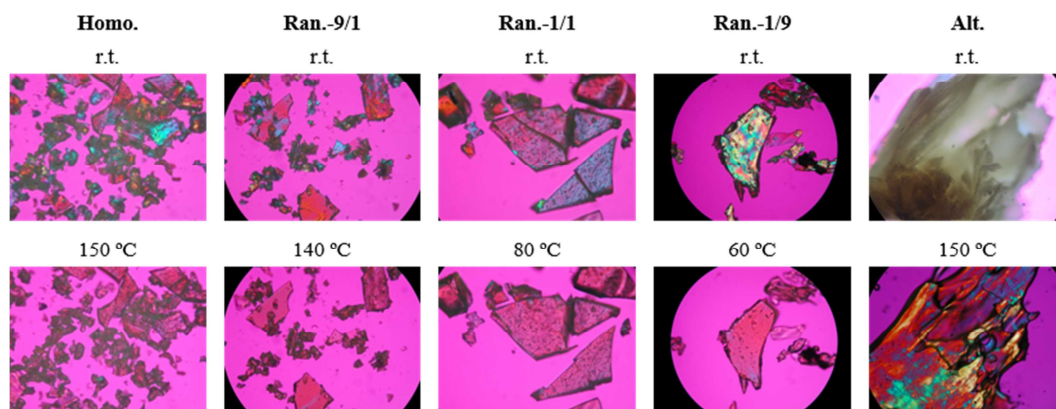


Figure S8. Polarized micrographs of the polymers in the solid state; at room temperature (top) and at 150 °C (**Homo.**), 140 °C (**Ran.-9/1**), 80 °C (**Ran.-1/1**), 60 °C (**Ran.-1/9**), and 150 °C (**Alt.**) (bottom).

Note: **Homo.** and **Ran.-9/1**, **-1/1**, **-1/9** showed textures indicative of liquid crystalline (LC) phase at r.t., but the textures almost disappeared on heating at the prescribed temperatures. On the other hand, while **Alt.** did not show any clear texture and was opaque at room temperature, it exhibited a clear texture at 150 °C. The polymer chains of **Homo.** and **Ran.-m/n** at room temperature seem to be aligned as obtained, and the alignment was not stable at an elevated temperature. In contrast, heating facilitates chain alignment of the alternating copolymer (**Alt.**).

Table S2. Optical properties: absorption maximum ($\lambda_{\text{Abs.max}}$), anisotropy factor in the ground state (g_{CD}), emission maximum ($\lambda_{\text{Em.max}}$), and internal fluorescence quantum yield (Φ_{Em}) of the polymers in a THF solution and in film and **NPF** in a THF solution.

	In a THF solution ^a				In film ^b			
	$\lambda_{\text{Abs.max}}$	$g_{\text{CD}} \times 10^4$	$\lambda_{\text{Em.max}}$	$\Phi_{\text{Em}}^{\text{c}}$	$\lambda_{\text{Abs.max}}$	$g_{\text{CD}} \times 10^4$	$\lambda_{\text{Em.max}}$	$\Phi_{\text{Em}}^{\text{c}}$
Homo.	373	-0.7	415	0.74	368	-1.1	438	0.39
Ran.-9/1	374	-0.5	415	0.74	369	-1.1	439	0.42
Ran.-1/1	375	-0.2	416	0.75	370	-0.5	439	0.42
Ran.-1/9	378	- ^d	417	0.76	376	-0.4	439	0.47
Alt.	384	- ^d	416	0.53	378	-0.2	422	0.03
Alt. (annealed ^e)	-	-	-	-	393	+260	520	0.04
NPF	270	-3.5	308	0.44	-	-	-	-

^aConc. = 1.0×10^{-5} M per residue, cell length = 1.0 cm, temp. = room temperature. ^bDrop-cast film on a quartz plate (size 1 cm \times 2 cm, thickness 1 mm). ^cInternal fluorescence quantum yield determined by using an integral sphere. ^dUnder the detection limit ($\text{CD} < \pm 0.04$ mdeg). ^eThe film was annealed at 160 °C for 48 h in the dark.

Note: Although the precise reason, why **Alt.** exhibits lower fluorescence quantum yields in both solution and film than the others, is not obvious at the present stage, the reason might come from structural flexibility of **Alt.**. The proposed structural flexibility of **Alt.** could facilitate a thermal relaxation of the excitation energy, resulting in the low fluorescence quantum yield of **Alt.**

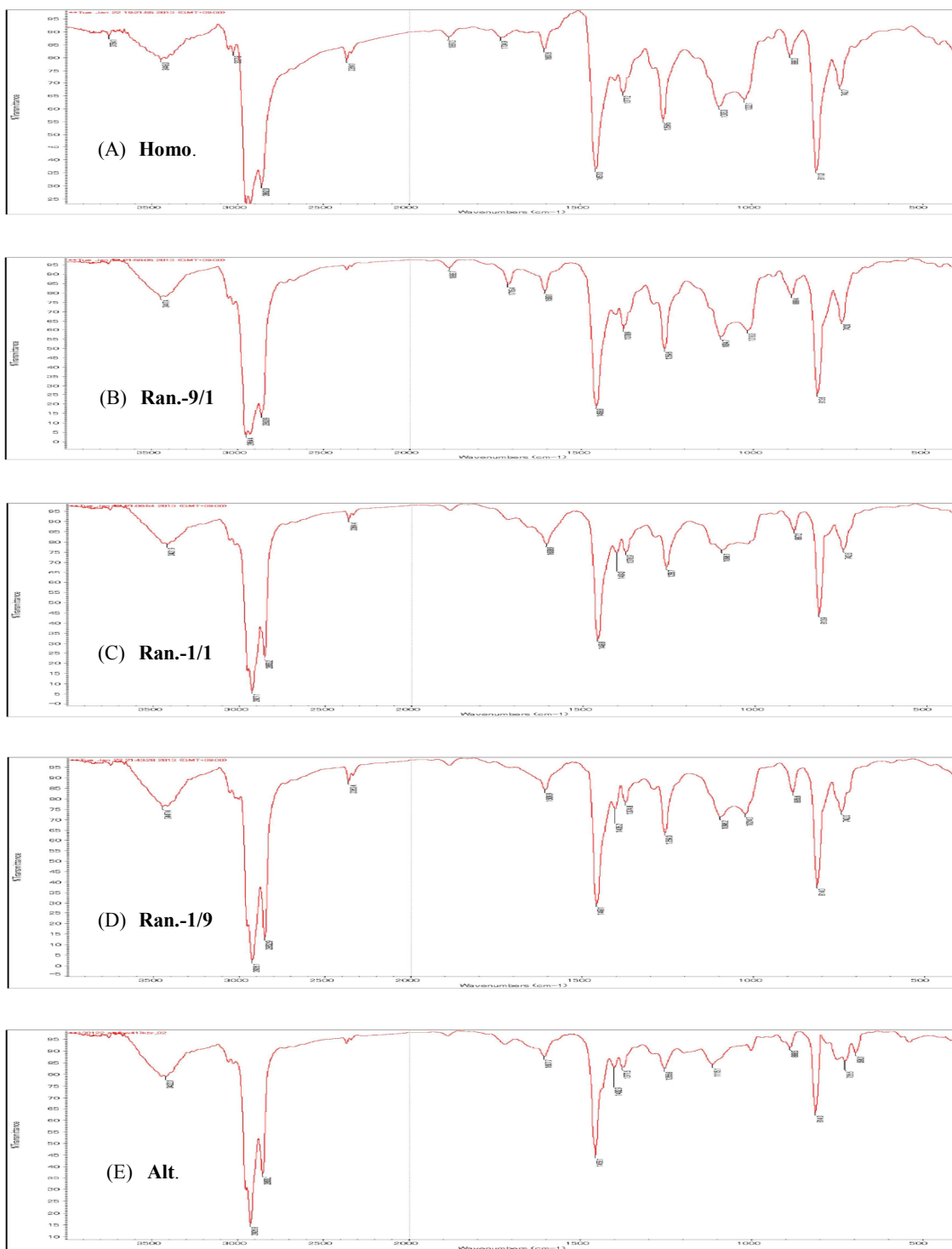


Figure S9. IR spectra of the homopolymer and the copolymers (KBr); **Homo.** (A), **Ran.-9/1** (B), **Ran.-1/1** (C), **Ran.-1/9** (D), and **Alt.** (E).

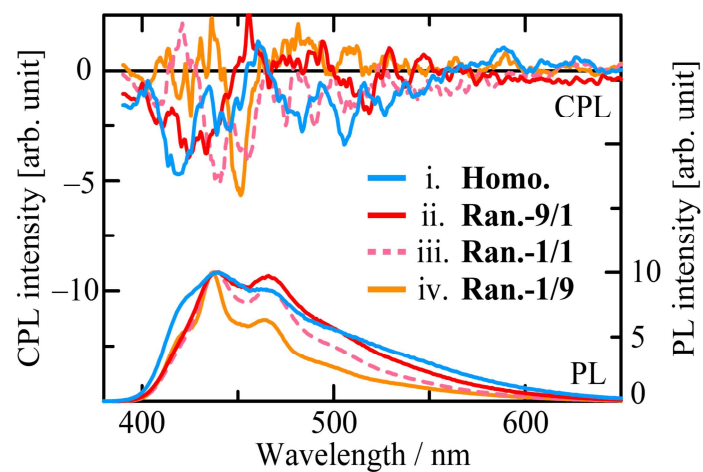


Figure S10. CPL and fluorescence (PL) spectra of thermally annealed films of the homopolymer and the random copolymers. λ_{ex} : in PL spectra, 366 nm for all the film samples; in CPL spectra, 350 nm for all the polymers.